AIP | Applied Physics Letters

Domain structure and in-plane switching in a highly strained Bi0.9Sm0.1FeO3 film

Weigang Chen, Wei Ren, Lu You, Yurong Yang, Zuhuang Chen, Yajun Qi, Xi Zou, Junling Wang, Thirumany Sritharan, Ping Yang, L. Bellaiche, and Lang Chen

Citation: Applied Physics Letters **99**, 222904 (2011); doi: 10.1063/1.3664394
View online: http://dx.doi.org/10.1063/1.3664394
View Table of Contents: http://scitation.aip.org/content/aip/journal/apl/99/22?ver=pdfcov
Published by the AIP Publishing

Domain structure and in-plane switching in a highly strained $Bi_{0.9}Sm_{0.1}FeO_3$ film

Weigang Chen,[1] Wei Ren,[2] Lu You,[1] Yurong Yang,[2,3] Zuhuang Chen,[1] Yajun Qi,[1] Xi Zou,[1] Junling Wang,[1] Thirumany Sritharan,[1] Ping Yang,[4] L. Bellaiche,[2] and Lang Chen[1,a)]
[1]*School of Materials Science and Engineering, Nanyang Technological University, Singapore 639798, Singapore*
[2]*Institute for Nanoscience and Engineering and Physics Department, University of Arkansas, Fayetteville, Arkansas 72701, USA*
[3]*Physics Department, Nanjing University of Aeronautics and Astronautics, Nanjing 210016, China*
[4]*Singapore Synchrotron Light Source (SSLS), National University of Singapore, 5 Research Link, Singapore 117603, Singapore*

(Received 20 September 2011; accepted 5 November 2011; published online 29 November 2011)

We report the domain structure and ferroelectric properties of a 32 nm-thick $Bi_{0.9}Sm_{0.1}FeO_3$ film epitaxially grown on a $LaAlO_3$ (LAO) substrate. This film exhibits a monoclinic *Mc* phase, with its monoclinic distortion and anisotropy of in-plane (IP) lattice parameters being both smaller than those of pure $BiFeO_3$ (BFO) grown on $LaAlO_3$. Polarization hysteresis loops measured using a quasi-planar capacitor show an *in-plane* polarization up to 30 $\mu C/cm^2$. Piezoresponse force microcopy demonstrates that a 180° *in-plane* polarization switching accompanied by a 90° domain wall rotation takes place after electric poling. First-principles calculations suggest the differences between highly strained Sm-substituted and pure $BiFeO_3$. © *2011 American Institute of Physics*. [doi:10.1063/1.3664394]

At room temperature, multiferroic $BiFeO_3$ (BFO) exhibits a rhombohedrally distorted (R) perovskite structure with a R3c space group.[1] In contrast with a R-like symmetry found in BFO films grown on substrates with relatively small lattice mismatches, a tetragonal-like (T-like) phase with a large axial ratio ($c/a \sim 1.24$) was observed in highly strained BFO films grown on $LaAlO_3$ (LAO), $LaSrAlO_4$ (LSAO), or $YAlO_3$ substrates.[2,3] Early, first-principle calculations suggested a tetragonal *P4mm* symmetry for that phase, with a giant polarization of 150 $\mu C/cm^2$ along the [001] direction.[4] Recent experiments rather revealed a monoclinic *Mc* phase with a polarization vector lying in the (100) plane in BFO films grown on LAO.[5,6] Based on polarization measurements of BFO films with mixed T-like and R-like phases, a spontaneous polarization of $\sim$150 $\mu C/cm^2$ was further deduced for the T-like phase.[7] The vertical ferroelectric switching of this T-like phase was also studied using piezoresponse force microscopy (PFM).[8] However, the polarization hysteresis loop for the pure T-like phase has not been reported so far because of the large leakage currents existing in the ultrathin films that possess the pure *Mc* phase. Furthermore, the exact polarization directions and the domain switching behavior of this *Mc* phase in BFO thin films are still not fully elucidated.

In addition to highly strained BFO, another topic of interest is about solid solutions made from the substitution of Bi by rare-earth elements (Re) in BFO.[9] The resulting material is denoted here as BReFO, with, e.g., Re = Sm, Gd, and Dy and exhibits a compositionally induced rhombohedral-to-orthorhombic phase transition, which is accompanied by enhanced electromechanical response and dielectric constant.[10,11] This structural transition was attributed to a chemical pressure originating from the ionic radii mismatch between Re and Bi.[11] Furthermore, it was recently reported that the Re substitution results in a continuous rotation of the polarization vector within the (110) plane in Sm-substituted BFO (BSFO) systems.[12]

An interesting issue currently unexplored is to combine epitaxial strains and BReFO compounds, which is to investigate properties of highly strained BReFO films, in general, and to reveal how they differ from those of pure BFO (if any), in particular. In this letter, we report structural and ferroelectric properties, as well as domain switching of a 10% Sm-substituted BFO thin film grown on a LAO substrate. First-principle calculations are also conducted to better understand the differences in properties between highly strained BFO and BSFO films.

A 32-nm-thick $Bi_{0.9}Sm_{0.1}FeO_3$ (BSFO) film was grown on a (001)-oriented LAO substrate.[13] BSFO film shows a homogeneous surface with a roughness of 0.37 nm. Topographic stripes, which were previously found in BFO films grown on LAO and LSAO because of multi-phase coexistence,[2,5] are absent, indicating that our film consists of a pure T-like phase. This is further confirmed by high resolution x-ray diffraction (HR-XRD) reciprocal space mappings (RSMs). The RSM around (002) shows only diffraction spots from the LAO substrate and the T-like phase (Fig. 1(a)). The (103) RSM of the T-like phase splits into three adjacent peaks: one peak is shifted up and another is shifted down with respect to the central peak (Fig. 1(b)), confirming that the T-like phase is monoclinic *Mc*. The structural parameters are determined to be: $a_m = 3.782 \pm 0.004$ Å and $b_m = 3.764 \pm 0.004$ Å for the in-plane (IP) lattice parameters, $c_m = 4.653 \pm 0.005$ Å for the out-of-plane (OP) lattice parameter, and the monoclinic angle β is equal to $89.4 \pm 0.1°$.[14] In comparison, for the *Mc* phase of pure BFO grown on LAO, the corresponding parameters are $a_m = 3.811$ Å, $b_m = 3.734$ Å, $c_m = 4.670$ Å, and $\beta = 88.2°$.[15]

a)Author to whom correspondence should be addressed. Electronic mail: langchen@ntu.edu.sg.

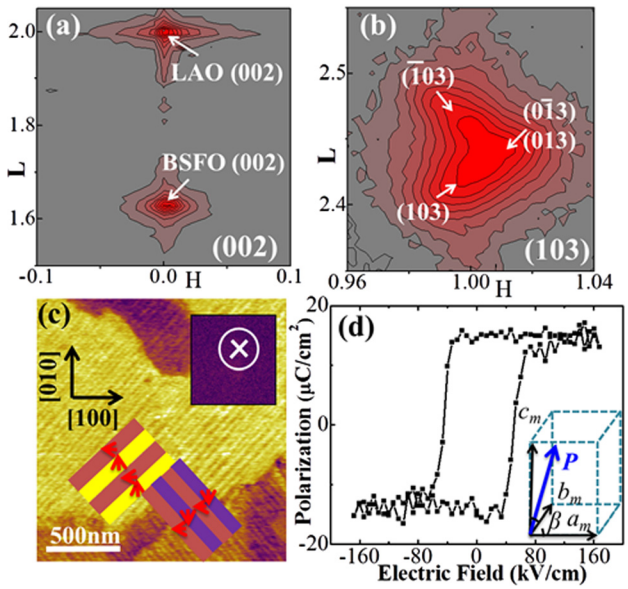

FIG. 1. (Color online) (a) and (b) HR-XRD RSMs near (002) and (103) of the *Mc* phase; (c) IP PFM image of the BSFO film with the tip cantilever aligned along the [100] direction. Upper inset is the OP PFM. Lower inset is the illustration of the arrangement of the IP polarization; (d) Remnant polarization hysteresis loop of the quasi-planar capacitor measured at 1 kHz. Inset is an illustration of the unit cell of the *Mc* phase.

In other words, the average in-plane lattice parameter is basically identical between BFO and BSFO grown on LAO, but the Sm substitution leads to a decrease in the anisotropy of the in-plane lattice parameters. Similarly, the monoclinic distortion is much smaller in BSFO than in BFO, as evidenced by the increase of the monoclinic angle towards 90° after the Sm substitution.

The split in the (103) RSM also suggests the existence of domain variants in the film, which is confirmed by PFM images. The OP PFM image shows uniform purple color, indicating that the OP polarization component is pointing downwards (upper inset of Fig. 1(c)). The IP PFM image, however, shows modulated stripe domains with three contrasts (purple, yellow, and brown) with domain walls aligned along the [110] or [1-10] directions (Fig. 1(c)). As the cantilever of the AFM tip was aligned parallel to the [100] direction of the LAO substrate, the IP polarization directions of purple and yellow domains are parallel to [0-10] and [010] directions, respectively, while the IP polarization direction in brown domains are parallel to either [100] or [-100] directions depending on the polarization directions in their adjacent domains. The arrangement of the IP polarization components is shown in the inset of Fig. 1(c).

Quasi-planar electrodes were patterned to measure the remnant polarization hysteresis loop.[13,16] The saturated *in-plane* polarization and the coercive field E_c are found to be 15 μC/cm^2 and 47.5 kV/cm, respectively (Fig. 1(d)). Because the IP electric field was applied along the [100] direction, domains with IP polarization component aligned perpendicular to the electric field will not contribute to the measured polarization. These domains correspond to purple or yellow regions which have an area percentage of 50% ± 7% in the IP PFM image (Fig. 1(c)). Thus, it is reasonable to estimate the total IP polarization to be 30 ± 5 μC/cm^2, which demonstrates that the polarization vector in the Mc phase BSFO is tilted away from the [001] OP direction with a non-negligible IP polarization component.

The ferroelectric domain structure within the quasi-planar channel was also monitored during the polarization switching cycle. After a voltage pulse (+60 V and 1 ms duration) is applied to the left electrode with electric field parallel to the [100] direction, brown domains align their net IP polarization along the electric field (Fig. 2(a)). The yellow/brown and purple/brown stripes correspond to the combinations of P_2/P_1 and P_4/P_1 domains, respectively, as shown in Fig. 2(b). When an opposite electric field is applied, the IP polarization of P_1 domains is switched by 180°. As a result, P_1 domains are switched to P_3 domains. P_2 and P_4 domains with IP polarization perpendicular to the electric field remain unchanged (Figs. 2(c) and 2(d)). Meanwhile, domain walls rotate 90° to avoid the formation of charged domain walls. However, OP PFM images showed no contrast change, irrespective of the polarity of the applied electric field. For the *Mc* phase of BFO—that has a polarization vector lying in the (100) plane[15]—the polarization vector can be switched in *five* possible ways (unlike the rhombohedral BFO which has three possible switching mechanisms, namely 71°, 109°, and 180° switching[17]). Three of them refer to the switching in which the OP polarization is switched by 180° while the IP polarization is switched by 0°, 90°, or 180°, respectively. The other two are pure IP switching in which only the IP polarization is switched by 90° or 180° correspondingly. In this study, only the 180° IP domain switching (with no OP

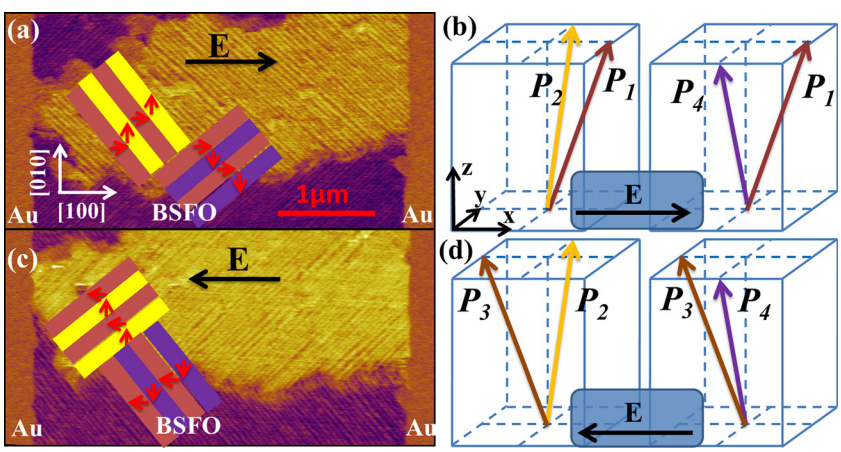

FIG. 2. (Color online) (a) and (b) are the IP PFM image and the illustration of polarization vectors after applying +60 V at the left electrode, respectively. (c) and (d) are the IP PFM image and the illustration of polarization vectors after applying −60 V. Insets in (a) and (c) are the illustrations of the IP domain arrangement with arrows indicating IP polarization directions. "E" denotes the applied electric field.

TABLE I. Physical properties of the BFO and BSFO films under an epitaxial strain of −4.5% from first principles calculations.

Physical properties	BFO	BSFO
40-atom cell lattice vectors divided by 2 (Å)	(3.800, 0.000, 0.000) (0.000, 3.800, 0.000) (0.208, 0.208, 4.821)	(3.800, 0.000, 0.000) (0.000, 3.800, 0.000) (0.119, 0.189, 4.786)
Polarization, C/m^2	(0.230, 0.230, 1.552)	(0.089,0.238, 1.554)
Antiferrodistortive vector, degree	(3.569, 3.569, 0.053)	(3.737, 3.553, 0.720)

switching) together with a 90° domain wall rotation are observed.

For a better understanding of the effect of Sm substitution, we also carried out *ab-initio* calculations on a BFO and a $Bi_{0.875}Sm_{0.125}FeO_3$ (ordered) system, both being under an epitaxial strain around −4.5% (Ref. 13) (note that the in-plane lattice parameters, a_m and b_m, are assumed to have the same magnitude in the calculations). Table I shows the predicted lattice vectors, as well as the Cartesian components of the polarization and of the antiferrodistortive (AFD) vector, in the *ground states* of BFO and BSFO films. The calculations yield a large tetragonal ratio of around 1.26 in both systems, with this ratio being slightly smaller in BSFO than in BFO. This is consistent with the aforementioned experimental results. On the other hand, the computations also predict that the considered highly strained BFO system exhibits a Cc phase with equal in-plane lattice parameters and polarization components, which disagrees with the Mc phase observed experimentally.[6,15] This disagreement may be due to the fact that grown BFO films exhibit two different in-plane lattice parameters, as a result of a possible elastic matching between different *Mc* domains.[18] Furthermore, the AFD vector of the oxygen octahedral motion in the predicted Cc phase of BFO almost vanishes along the OP [001] direction and is around 5° along the IP [110] direction. Note that highly strained BSFO also possesses AFD motions, with similar IP components and a slightly larger OP component as compared with those of pure BFO. Moreover, the Cartesian components of the polarization component along the [010] direction ($\sim 24\ \mu C/cm^2$) is much larger than that along the [100] direction ($\sim 9\ \mu C/cm^2$) in BSFO—which is consistent with the *Mc* phase experimentally reported here for this system—while pure BFO is predicted to have equal IP polarization components ($\sim 23\ \mu C/cm^2$). In other words, the IP polarization rotates from nearly [110] for BFO to nearly [010] for BSFO with the angle made by the polarization vector and the [001] direction decreasing from 12° for pure BFO to around 9° for BSFO, which is consistent with the decrease in the monoclinic angle experimentally discovered here when going from BFO to BSFO films grown on LAO. To understand this rotation, we further decomposed the polarization inside each of the eight unit cells forming the BSFO supercell. Interestingly, the unit cell containing Sm and one of its neighboring unit cells along the y-axis are found to both have x-components of the local dipole moments aligned antiparallel to those of the 6 other unit cells, which nearly cancels the total component of the polarization along the [100] pseudo-cubic direction. This antipolar-like order may be a precursor of the antiferroelectric-like regions found in bulk-like BSFO systems when the Sm concentration is increased beyond 14%.[10,19]

In summary, remnant polarization hysteresis loops obtained for a *Mc* phase in BSFO films show a large IP polarization of $\sim 30\ \mu C/cm^2$. Combining the IP domain images and switching mechanisms for the *Mc* phase, we conclude that a 180° IP polarization switching accompanied by a 90° domain wall rotation occur in the BSFO film. First-principles calculations further provide some insights into the difference of ferroelectric properties between highly strained BFO and BSFO films.

L.C. acknowledges MINDEF-NTU-JPP 10/12 and NRF CREATE HUJ-BGU–NTU. P.Y. acknowledges SSLS via NUS Core Support C-380-003-003-001. W.R., Y.Y., and L.B. acknowledge NSF grant DMR-1066158 and the Department of Energy, Office of Basic Energy Sciences, under Contract No. ER-46612. They also acknowledge NSF Grant No. DMR-0701558 and ONR Grant Nos. N00014-11-10384 and N00014-08-1-0915 for discussions with scientists sponsored by these grants. Some computations were possible thanks to the MRI Grant No. 0959124 from NSF, N00014-07-1-0825 (DURIP) from ONR and a Challenge grant from HPCMO of the U.S. Department of Defense.

[1]N. A. Spaldin, S. W. Cheong, and R. Ramesh, Phys. Today **63**, 38 (2010).
[2]R. J. Zeches, M. D. Rossell, J. X. Zhang, A. J. Hatt, Q. He, C. H. Yang, A. Kumar, C. H. Wang, A. Melville, C. Adamo *et al.*, Science **326**, 977 (2009).
[3]H. Béa, B. Dupé, S. Fusil, R. Mattana, E. Jacquet, B. Warot-Fonrose, F. Wilhelm, A. Rogalev, S. Petit, V. Cros, A. Anane *et al.*, Phys. Rev. Lett. **102**, 217603 (2009).
[4]C. Ederer and N. A. Spaldin, Phys. Rev. Lett. **95**, 257601 (2005).
[5]Z. H. Chen, L. You, C. W. Huang, Y. J. Qi, J. L. Wang, T. Sritharan, and L. Chen, Appl. Phys. Lett. **96**, 252903 (2010).
[6]H. M. Christen, J. H. Nam, H. S. Kim, A. J. Hatt, and N. A. Spaldin, Phys. Rev. B **83**, 144107 (2011).
[7]J. X. Zhang, Q. He, M. Trassin, W. Luo, D. Yi, M. D. Rossell, P. Yu, L. You, C. H. Wang, C. Y. Kuo *et al.*, Phys. Rev. Lett. **107**, 147602 (2011).
[8]D. Mazumdar, V. Shelke, M. Iliev, S. Jesse, A. Kumar, S. V. Kalinin, A. P. Baddorf, and A. Gupta, Nano. Lett. **10**, 2555 (2010).
[9]S. Fujino, M. Murakami, V. Anbusathaiah, S. H. Lim, V. Nagarajan, C. J. Fennie, M. Wuttig, L. Salamanca-Riba, and I. Takeuchi, Appl. Phys. Lett. **92**, 202904 (2008).
[10]I. Levin, S. Karimi, V. Provenzano, C. L. Dennis, H. Wu, T. P. Comyn, T. J. Stevenson, R. I. Smith, and I. M. Reaney, Phys. Rev. B **81**, 020103 (2010).
[11]D. Kan, L. Palova, V. Anbusathaiah, C. J. Cheng, S. Fujino, V. Nagarajan, K. M. Rabe, and I. Takeuchi, Adv. Funct. Mater. **20**, 1108 (2010).
[12]D. Kan, V. Anbusathaiah, and I. Takeuchi, Adv. Mater. **23**, 1765 (2011).
[13]See supplementary material at http://dx.doi.org/10.1063/1.3664394 for detailed experimental and calculation methods.
[14]F. M. Bai, N. G. Wang, J. F. Li, D. Viehland, P. M. Gehring, G. Y. Xu, and G. Shirane, J. Appl. Phys. **96**, 1620 (2004).
[15]Z. H. Chen, Z. L. Luo, C. W. Huang, Y. J. Qi, P. Yang, L. You, C. S. Hu, T. Wu, J. L. Wang, C. Gao *et al.*, Adv. Funct. Mater. **21**, 133 (2011).
[16]L. You, E. Liang, R. Guo, D. Wu, K. Yao, L. Chen, and J. L. Wang, Appl. Phys. Lett. **97**, 062910 (2010).
[17]F. Zavaliche, P. Shafer, R. Ramesh, M. P. Cruz, R. R. Das, D. M. Kim, and C. B. Eom, Appl. Phys. Lett. **87**, 252902 (2005).
[18]Z. H. Chen, S. Prosandeev, Z. L. Luo, W. Ren, Y. J. Qi, C. W. Huang, L. You, C. Gao, I. A. Kornev, T. Wu *et al.*, Phys. Rev. B **84**, 094116 (2011).
[19]C. J. Cheng, D. Kan, S. H. Lim, W. R. McKenzie, P. R. Munroe, L. G. Salamanca-Riba, R. L. Withers, I. Takeuchi, and V. Nagarajan, Phys. Rev. B **80**, 014109 (2009).